Impact of the Precision in NMR Relaxation Measurements on the Interpretation of Protein Dynamics

Danqing Jin,[†] Francisco Figueirido,[†]
Gaetano T. Montelione,[‡] and Ronald M. Levy*,[†]

Rutgers, The State University of New Jersey
Piscataway, New Jersey 08855-0939

Received March 25, 1997
Revised Manuscript Received May 4, 1997

NMR relaxation (T_1, T_2, NOE) experiments are a very important tool for studying the internal dynamics of proteins.[1,2] Molecular information can be extracted from the relaxation data using various analytical models for the dynamics whose parameters are derived from fits to the relaxation data.[3] Another approach involves the direct mapping of spectral density functions from experimental data.[4] The approach most commonly used is based on the so-called "model-free" formalism.[5,6] The information contained in the relaxation data is assumed to be completely specified by two quantities: a generalized order parameter, S^2, which is a measure of the spatial restriction of the internal motion, and an effective correlation time, τ_e, which is a measure of the rate of the internal motion. This framework has been applied by a number of groups to interpret NMR relaxation experiments on proteins.[7−11]

The model-free parameters are usually extracted by minimization of an error function which is a measure of the difference between the calculated and experimental relaxation parameters.[8] Although this fitting procedure has been widely applied, the effects of the precision in the measured NMR parameters on the theoretical parameters is far from transparent. As we demonstrate here, the information contained in the NMR experiments concerning dynamics is rapidly degraded as the uncertainties in the NMR relaxation measurements grow.

In this communication we show how the complete set of model-free parameters consistent with the experimental data can be determined graphically. The procedure is applied to published data[11] to demonstrate the effect of experimental uncertainties on motional parameters in different regimes. We note that the graphical method has been applied previously in a more limited way to extract protein order parameters and effective correlation times from NMR experiments.[12]

The heteronuclear relaxation of protonated ^{15}N nuclei is mediated primarily by dipole−dipole interactions with the attached protons and secondarily by chemical shift anisotropy. The relaxation rates depend on spectral density functions which contain the dynamical information. In the "model-free" formalism,[5] the spectral density function, assuming isotropic overall tumbling, is characterized by the two parameters, S^2 and τ_e. The expression for $J(\omega)$ is

$$J(\omega) = \frac{2}{5}\left[\frac{S^2\tau_m}{1+(\omega\tau_m)^2} + \frac{(1-S^2)\tau}{1+(\omega\tau)^2}\right] \quad (1)$$

where $1/\tau = 1/\tau_e + 1/\tau_m$ and τ_m is the overall correlation time of the macromolecule of interest. The only requirements for the validity of the "model-free" expression for the spectral density are that the overall tumbling and the internal motions be uncoupled and that the correlation functions describing these motions decay as single exponentials. In particular, we note that there is no requirement that the internal motions be close to the extreme narrowing limit, although as discussed below, the way in which the precision in the experimental measurements propagates through to the precision in the derived model-free parameters is affected by the relative time scales of the internal and tumbling motions.

When τ_m is determined for the macromolecule, R_1 can be directly calculated if S^2 and τ_e are given, whereas it is not possible to evaluate S^2 or τ_e analytically even if the relaxation rates R_1, R_2, and NOE are known. Longitudinal relaxation data may be written in the form $R_1 \pm \Delta R_1$, where ΔR_1 corresponds to the uncertainty in the measurements. The essence of our graphical procedure involves the construction of contour lines of constant R_1 as a function of S^2 and τ_e. For a given relaxation measurement with its estimated error, the area in the (S^2,τ_e) plane between the two contour lines defined by $R_1 - \Delta R_1$ and $R_1 + \Delta R_1$ contains all pairs of (S^2,τ_e) parameters consistent with the experimental measurement. By the same procedure, regions in the (S^2,τ_e) plane containing model-free parameters consistent with the transverse relaxation and NOE measurements can be determined. The overlap of these areas defines the complete solution space for the model-free parameters that contain (S^2,τ_e) pairs which are consistent with all three NMR relaxation measurements.

Contour maps of R_1, R_2, and NOE are displayed in Figure 1. For each of the NMR relaxation parameters, regions where the contour lines are most densely spaced correspond to regions of (S^2,τ_e) space which are least sensitive to errors in the measured parameters. For both R_1 and NOE, there is a large variation in the spacing of the contour lines in different regions of the contour map, with the most densely spaced region corresponding to small order parameters S^2 coupled with short internal correlation times τ_e; the spacing of spin−spin relaxation R_2 contour lines as a function of (S^2,τ_e) is more uniform. For illustrative purposes, the shaded area on each contour map indicates the allowed values of (S^2,τ_e) corresponding to a representative set of NMR relaxation parameters (see the figure legend). The shaded region in Figure 1d contains the pairs (S^2,τ_e) which are consistent with all the NMR relaxation data, corresponding to the superposition of the shaded regions in 1a−c. Note that the shaded region in Figure 1d containing the set of solutions (S^2,τ_e) consistent with all the relaxation data is not rectangular as would be the case if the uncertainties in the two model-free parameters were independent of each other. In the literature however, the errors in S^2 and in τ_e are usually reported as independent quantities.

[†] Department of Chemistry.
[‡] Department of Molecular Biology and Biochemistry and Center for Advanced Biotechnology and Medicine.
* Corresponding author. Phone: (908) 445-3947. FAX: (908) 445-5958. E-mail: ronlevy@lutece.rutgers.edu.

(1) Abragam, A. *The Principles of Nuclear Magnetism*; The International Series of Monographs on Physics; Oxford University Press: Oxford, 1961.
(2) London, R. E. *Magnetic Resonance in Biology*; John Wiley & Sons: New York, 1980; Vol. 1, pp 1−69.
(3) Woessner, D. E. *J. Chem. Phys.* **1962**, *37*, 647−654. Wallach, D. J. *J. Chem. Phys.* **1967**, *47*, 5258. Wittebort, R. J.; Szabo, A. *J. Chem. Phys.* **1978**, *69*, 1722. Brainard, J. R.; Szabo, A. *Biochemistry* **1981**, *20*, 4618. Levy, R. M.; Karplus, M.; Wolynes, P. G.; *J. Am. Chem. Soc.* **1981**, *103*, 5998−6011. Levy, R. M.; Sheridan, R. P. *Biophys. J.* **1983**, *41*, 217−221. Bremi, T.; Bruschweiler, R.; Earnst, R. R. *J. Am. Chem. Soc.* **1997**, in press.
(4) Peng, J. W.; Wagner, G. *J. Magn. Reson.* **1992**, 98, 308−332.
(5) Lipari, G.; Szabo, A. *J. Am. Chem. Soc.* **1982**, *104*, 4546−4559.
(6) Levy, R. M.; Karplus, M.; McCammon, J. A. *J. Am. Chem. Soc.* **1981**, *103*, 994−996. Clore, G. M.; Szabo, A.; Bax, A.; Kay, L. E.; Driscoll, P. C.; Gronenborn, A. M. *J. Am. Chem. Soc.* **1990**, *112*, 4989−4991. Clore, G. M.; Driscoll, P. C.; Wingfield, P. T.; Gronenborn, A. M. *Biochemistry* **1990**, *29*, 7387−7401.
(7) Kay, L. E.; Torchia, D. A.; Bax, A. *Biochemistry* **1989**, *28*, 8972−8979.
(8) Palmer, A. G., III; Rance, M.; Wright, P. E. *J. Am. Chem. Soc.* **1991**, *113*, 4371−4380.
(9) Kay, L. E.; Nicholson, L. K.; Delaglio, F.; Bax, A.; Torchia, D. A. *J. Magn. Reson.* **1992**, *97*, 359−375. Kordel, J.; Skelton, N. J.; Akke, M.; Palmer, A. G., III; Chazin, W. J. *Biochemistry* **1992**, *31*, 4856−4866. Powers, R.; Clore, G. M.; Stahl, S. J.; Wingfield, P. T.; Gronenborn, A. M. *Biochemistry* **1992**, *31*, 9150−9157.
(10) Stone, M. J.; Fairbother, W. J.; Palmer, A. G., III; Reizer, J.; Saier, M. H.; Wright, P. E. *Biochemistry* **1992**, *31*, 4394−4406.
(11) Li, Y.; Montelione, G. T. *Biochemistry* **1995**, *34*, 2408−2423.
(12) Henry, G. D.; Weiner, J. H.; Skyes, B. D. *Biochemistry* **1986**, *25*, 590−598. Weaver, A. J.; Kemple, M. D.; Prendergast, F. G. *Biophys. J.* **1988**, *54*, 1−15.

S0002-7863(97)00947-5 CCC: $14.00

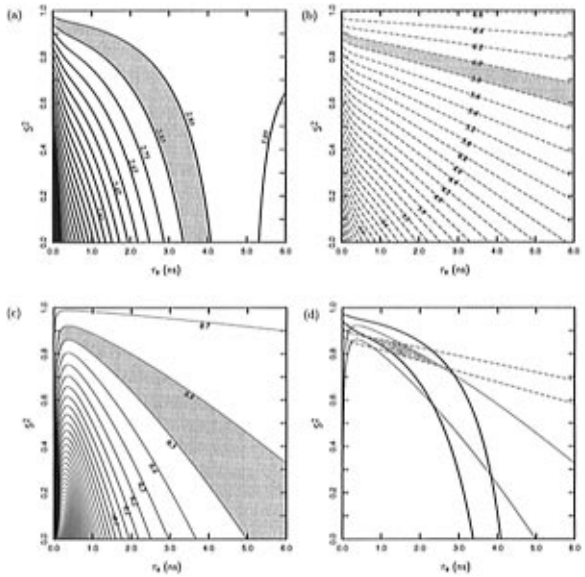

Figure 1. Contour maps of S^2 and τ_e for different types of ^{15}N NMR relaxation measurements: (a) longitudinal R_1 contours; (b) transverse R_2 contours; (c) heteronuclear NOE contours [For these contour maps, the spectrometer frequencies ω_H and ω_N were chosen to be 500 and 50.7 MHz, respectively, and the overall correlation time 4 ns. To illustrate the mapping procedure, a region is shaded in each map corresponding to the following sample NMR data: $R_1 = 2.88 \pm 0.05$ s^{-1}, $R_2 = 5.90 \pm 0.10$ s^{-1}, NOE $= 0.55 \pm 0.05$]; (d) superposition of the allowed (S^2,τ_e) pairs from Figure 1a−c. Contour lines for R_1, R_2, and NOE are denoted as thick lines, dashed lines, and thin lines, respectively.

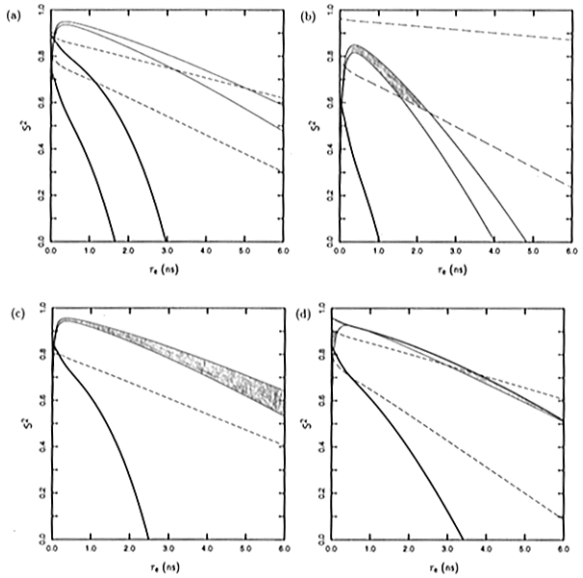

Figure 2. Application of the graphical method to published[11] backbone $^{15}N-^{1}H$ NMR relaxation data for the protein hTGFα (Figure 2a−c) and unpublished data for a PTI [C30V, C51A] mutant (Figure 2d). The $S^2-\tau_e$ solution spaces are indicated by shaded area(s) in each plot. The experimental relaxation data are (a) hTGFα Ala-31: $R_1 = 2.50 \pm 0.22$ s^{-1}, $R_2 = 5.36 \pm 0.29$ s^{-1}, NOE $= 0.62 \pm 0.01$; (b) hTGFα Asn-6: $R_1 = 2.61 \pm 0.71$ s^{-1}, $R_2 = 5.53 \pm 0.58$ s^{-1}, NOE $= 0.44 \pm 0.03$; (c) hTGFα Tyr-38: $R_1 = 2.83 \pm 0.23$ s^{-1}, $R_2 = 5.85 \pm 0.59$ s^{-1}, NOE $= 0.63 \pm 0.01$; (d) PTI mutant Phe-4: $R_1 = 2.79 \pm 0.19$ s^{-1}, $R_2 = 4.25 \pm 0.30$ s^{-1}, NOE $= 0.56 \pm 0.07$. Contour lines for R_1, R_2, and NOE are denoted as those in Figure 1.

The graphical procedure for determining model-free parameters described in this communication was applied (see Figure 2a−c) to representative experimental data from NMR relaxation studies of the dynamics of human type-α transforming growth factor (hTGFα) reported by Li and Montelione.[11] For the backbone NH bond of residue Ala-31 (Figure 2a), the graphical solutions ($S^2 = 0.83$, $\tau_e = 55$ ps) agree very well with the numerical solutions obtained by repeated optimizations of an error function starting from different initial conditions.[8] The graphical solutions for the model-free parameters consistent with the experimental NMR data for the NH bond of Asn-6 are shown in Figure 2b. The agreement with the solutions for (S^2,τ_e) obtained by optimizing the error function reported in ref 11 is relatively poor. The values reported for S^2 and τ_e for Asn-6 were 0.83 ± 0.06 and 0.52 ± 0.43 ns, respectively, while actually the set of solutions (S^2,τ_e) consistent with the experimental data found by the graphical method are highly correlated, S^2 varies between 0.56 and 0.85, while τ_e varies between 0.1 and 2.3 ns (see Figure 2b).

A striking example of the disagreement between the graphical method and the numerical procedure based on minimization for finding model-free parameters is provided by the NMR relaxation data for the backbone NH bond of Tyr-38 (see Figure 2c). Model-free parameters consistent with the experimental data were located by the numerical method, but the method does not provide a reliable estimate of the size of the solution space. The generalized order parameters and effective correlation times determined by minimization of the error function were reported to be $S^2 = 0.91 \pm 0.01$ and $\tau_e = 108 \pm 24$ ps.[11] However, according to the graphical analysis (Figure 2c), the uncertainties in the NMR relaxation measurements are sufficiently large, so that little useful information about the motion of the NH backbone of Tyr-38 can be extracted from these measurements. Shown in Figure 2c are correlated (S^2,τ_e) pairs consistent with the experimental data; S^2 varies between 0.55 and 0.95, while τ_e varies between 0.1 and 6 ns. Although not shown in the figure, there are additional solutions to the model-free equations with even smaller order parameters and larger effective correlation times. Thus, for both Asn-6 and Tyr-38, the size of the model-free parameter space consistent with the relaxation data is much larger than the set determined by the numerical optimization procedure. Interestingly, the amount of molecular information about protein motions contained in the NMR relaxation data depends both on the relative uncertainty in the measurements *and* on the absolute values of the relaxation rates; the rates in turn depend both on the overall tumbling time and the spectrometer frequency.

Figure 2d presents a final example of the graphical analysis of NMR relaxation data based on unpublished experiments on a mutant form of pancreatic trypsin inhibitor (PTI). The measured relaxation data are reported in the legend. The example was included to show the possibility of finding discontinuous regions in (S^2,τ_e) space which are consistent with the experimental data for some combinations of NMR relaxation parameters. For this data set, there are (S^2,τ_e) pairs which fit the experimental data with large order parameters and very short effective correlation times as found by the error function analysis and also by the graphical method. However, as shown in Figure 2d, there is another set of solutions to the equations with much smaller order parameters and larger effective correlation times. It should be noted that the solutions to the "model-free" equations shown in Figures 2b−d which fit the experimental data do not depend on the assumption that $\tau_e \ll \tau_m$. However, for a fixed precision in the experimental measurements, the precision in the model-free parameters is coupled to the separation between τ_e and τ_m.[5] For cases where there are discontinuous sets of solutions to the model-free equations, it should be possible to determine the physically correct set of solutions by carrying out additional relaxation experiments at multiple field strengths. A complete graphical analysis of these issues as well as application of the method to the "extended" model-free formalism will be presented elsewhere.

Acknowledgment. This work was supported by a grant from the National Institutes of Health (NIH GM30580).

JA970947+